Aqueous Catalytic Disproportionation and Oxidation of Nitric Oxide

4 **AUTHORS**, INCLUDING:

Joseph Macneil
Chatham University

28 PUBLICATIONS **277** CITATIONS

SEE PROFILE

William C. Trogler
University of California, San Diego

249 PUBLICATIONS **7,825** CITATIONS

SEE PROFILE

Aqueous Catalytic Disproportionation and Oxidation of Nitric Oxide

J O S E P H   H.   M A C N E I L,
P O L L Y   A.   B E R S E T H,
G L E N N   W E S T W O O D,   A N D
W I L L I A M   C.   T R O G L E R *

Department of Chemistry and Biochemistry, University of California at San Diego, La Jolla, California 92093-0358

Nitric oxide, a byproduct of combustion exhaust, is a key species that leads to urban photochemical smog. Nitric oxide exhibits low aqueous solubility, and it has proved difficult to remove NO from gas streams by aqueous scrubbing methods. A catalyst for the aqueous disproportionation of NO to nitrous oxide and aqueous nitrite has been developed with wood-derived activated carbons. Addition of palladium or platinum metal to the carbon support significantly accelerates catalysis. The carbon-supported catalyst was not poisoned by sulfur oxides. The reaction is thought to involve the reduction of surface-bound nitric oxide dimers. The reducing equivalents stem from the oxidation of NO to NO_2^-. Addition of oxygen as an alternative electron acceptor during the reaction immediately arrested nitrous oxide formation, and all the nitric oxide was removed from the gas stream as aqueous nitrite. This demonstrates the feasibility of removing SO_x and NO_x simultaneously by low-temperature aqueous scrubbing.

Introduction

Because of nitrogen oxide's key role in photochemical smog and in acid rain formation, NO_x controls are a priority in urban regions (*1*). In the United States, the 1990 Clean Air Act Amendments mandated stringent NO_x emissions reductions. Stationary combustion sources, primarily electric power plants, generate large amounts of NO_x byproducts that account for more than half the total U.S. NO_x emissions. Emerging legislation for zero-emission vehicles (electric cars) will further shift the NO_x burden onto stationary combustion sources.

The implementation of postcombustion technologies is especially problematic for coal-fired utilities. Selective catalytic reduction (SCR) of NO by NH_3 at 300−400 °C is the best available NO_x control technology for stack gases (*2*); however, difficulties with fly ash poisoning, ammonia slippage, and high overall operating expenses have prompted a search for alternative methods. Selective noncatalytic reduction (SNCR) of NO_x to N_2, employing ammonia or urea, is also in use. This requires operating temperatures in the range 800−1200 °C. Emission reduction levels of 50−70% are typically obtained with this process. Attention has also focused on decomposing NO to N_2 and O_2 by Cu-doped ZSM-5 zeolites and related systems (*3, 4*); however, these are not yet viable for stationary combustion sources.

Noncatalytic oxidation/reduction and absorption techniques (chemical scrubbing) have the advantage of being able to eliminate both NO_x and SO_x simultaneously (*5, 6*). The primary impediment to their industrial application has been the low solubility of NO in aqueous solution. Because nitric oxide is 90−95% of the NO_x present in typical flue gas streams (*7*), it has been necessary to preoxidize NO to NO_2 before the scrubber. Direct oxidation with O_2 occurs slowly at the low NO concentrations present in exhaust streams. The additional complexity and expense of using alternative oxidants, such as OCl^- and H_2O_2, have prevented widespread use of this method. Other approaches to treating NO in aqueous scrubbers have included the addition of heavy metal chelators to sequester nitric oxide for subsequent removal (*8*) and even the addition of yellow phosphorus emulsions and O_2 to oxidize nitric oxide to a combination of nitrite and nitrate salts (*9*).

In this paper we report a novel catalytic approach for removing NO in aqueous solution with supported palladium or platinum metal. The catalysts display activity at ambient temperatures and are not poisoned by SO_2.

Experimental Section

Reactions were performed with standard Schlenk techniques under anaerobic conditions, except where it is noted otherwise. UV/vis spectra were recorded with an HP 8452A diode array spectrometer in 1.0 cm quartz cells. IR data were acquired at 2 cm^{-1} resolution with a Nicolet 510 FTIR spectrometer fitted with a MCT liquid nitrogen-cooled detector. Pyrex cells with CaF_2 windows and 5 or 10 cm path lengths were used for gas sampling. Gas chromatograph (GC) analyses were performed with the use of a Hewlett-Packard 5890 GC that was fitted with a 6 ft × 1/8 in. o.d. 13× molecular sieve column (45/60 mesh) and a thermal conductivity detector. Data were output to a HP-3392A integrator. The NO (Liquid Air, 99% min purity) used in the majority of the experiments was spectroscopically free (<5 ppm) of higher nitrogen oxides but contained trace quantities of N_2O. Dilute nitric oxide (Matheson, 0.493% in NO, 1 ppm NO_2) was used for the recirculation experiments. Liquid nitrogen boil-off was the source of gaseous N_2. Aqueous solutions were prepared with degassed HPLC-grade water. The following wood-derived activated carbons (used as received from commercial suppliers) were tested: Darco granular (20−40 mesh), Darco KB (100 mesh), Darco-KB-B (<100 mesh), Darco G-60, Norit SA3 (<100 mesh), and Engelhard CP-97. Palladium (0.5%, 1%, 5%, 10%) on activated carbon, platinum (0.5%, 3%) on activated carbon, Pearlman's catalyst [20% $Pd(OH)_2$ on carbon], and Lindlar catalyst (5% Pd on $CaCO_3$) were obtained from Aldrich. $PdCl_2$, palladium (5%, 10%) on carbon, palladium (0.5%) on alumina, and palladium(II) (5%) on barium sulfate were obtained from Strem Chemicals, Inc.

Standard Reaction Conditions. A Schlenk flask containing 0.10 g of catalyst in 10.0 mL of 3 M NaOH was pressurized to 840 Torr with NO (350 mL of headspace). Rapid stirring was used to facilitate NO uptake into the aqueous phase. The flask was repressurized with argon as the NO was depleted. The course of the reaction was monitored by periodic GC analysis of 50-μL samples extracted from the headspace. Calibration curves were used to determine the relative quantities of NO, N_2O, and argon in each sample. The temperature was 22 °C for all the rates reported herein, unless otherwise noted.

Low NO Concentrations. Recirculation reactions were performed in a closed loop system consisting of the reactor

* Corresponding author telephone: 619-534-6175; fax: 619-534-5383; e-mail: wtrogler@ucsd.edu.

vessel, a gas-phase IR cell, and a peristaltic recirculation pump linked by Tygon tubing. The system was evacuated and purged three times with nitrogen, before filling with 1000–6000 ppm NO. Nitrogen was used to bring the final pressure up to 780 Torr. In some experiments O_2 (1–5%) was also added. The rate of reaction at 22 °C was monitored by FTIR spectroscopy; both the depletion of NO and the increase in N_2O were calculated from calibration curves. Complete recirculation of the headspace volume occurred every 45–50 s. Varying the recirculation rate did not change the reaction rate, which implies that NO saturation of the aqueous phase was maintained.

Preparation of an Activated Carbon-Supported Palladium Catalyst. Palladium dichloride (0.4936 g) was dissolved in 50.0 mL of 0.20 M HCl and stirred with 4.08 g of activated carbon (Engelhard) for 65 h. After extraction of a small aliquot for UV/vis analysis, the solution was filtered, and the precipitate was washed with HPLC-grade water until the supernatant was free of chloride (tested with $AgNO_3$). The palladium concentrations of the solution immediately before filtration and after washing were determined from UV/vis analyses at 474 nm ($\epsilon_{max\ (PdCl_4)^{2-}} = 160 \pm 10$ cm^{-1} M^{-1}). A total of 0.274 g of palladium had been adsorbed by the carbon, corresponding to 6.7 wt %. The sample was dried overnight under vacuum. A 1.0-g sample of the $PdCl_2$-treated carbon was added to 25 mL of 3 M NaOH and shaken under 3 atm of H_2 for 18 h. The Pd^0/C product was filtered and dried under vacuum.

Calculation of Turnover Data. As indicated in the discussion to follow, 4 mol of nitric oxide was required to produce 1 mol of N_2O (and 2 mol of nitrite). The nitrite stoichiometry was determined by purging NO and N_2O from the solution with N_2 and filtering the reaction solution through a syringe tip filter to remove catalyst. An aliquot was diluted 25-fold with 1 M NaOH, and the concentration of NO_2^- was determined from its UV absorption maximum at 354 nm using a calibration curve for $NaNO_2$ constructed for the range 0.002–0.1 M. Turnover data were calculated as [(moles of N_2O × 4)/moles of palladium]. This rate, based on the product formation data, eliminated overestimation in the reactant disappearance rate, which results from adsorption of NO onto the heterogeneous component. This is evident by a rapid initial uptake of NO from the gas headspace before any product formation occurs. In the absence of the heterogeneous component, NO has very low solubility in water, and the amount removed from the headspace by dissolution is insignificant. The N_2O product absorbs much less strongly to the heterogeneous support.

Results

Anaerobic Experiments. The decomposition of nitric oxide is thermodynamically favorable, but it is slow under most conditions. Attention has focused on catalysts that drive the decomposition toward N_2 and O_2 (*3, 4*). While some notable success has been achieved, the use of elevated temperatures has proven unavoidable. We have observed that, in the absence of oxygen, basic aqueous solutions slowly promote the disproportionation of NO via eq 1 at ambient temperatures. Under the standard reaction conditions (22 °C, 10 mL of 3 M NaOH, 840 Torr of NO) employed, this background rate was 5.0×10^{-7} mol of N_2O/min or 20×10^{-7} mol of NO/min.

$$4NO + 2OH^- \rightarrow N_2O + 2\ NO_2^- + H_2O \qquad (1)$$
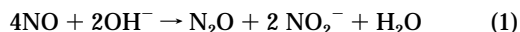
Reaction 1 is catalyzed by a slurry of activated carbon and further accelerated by palladium-treated activated carbons. Mass balance experiments are consistent with the stoichiometry of reaction 1 in all instances. Figure 1 depicts the relative rates of reaction.
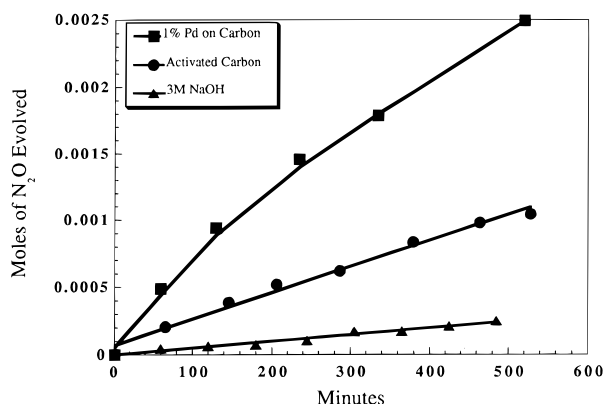

FIGURE 1. Catalytic enhancement of the rate of eq 1 by activated carbon and by 1% palladium-loaded activated carbon. Rates are given as moles of N_2O product formed vs reaction time (0.1 g of catalyst, 10 mL of 3 M NaOH, 840 Torr of NO, 22 °C).

TABLE 1. Rates (22 °C) of NO Disproportionation Catalyzed by Various Activated Carbons in 3 M NaOH with 840 Torr of NO

carbon sample	(mol of NO) min^{-1} (g of C)$^{-1}$
Darco Granular	10×10^{-5}
Darco KB	7.2×10^{-5}
Darco KB[a]	10×10^{-5}
Darco KB-B	8.4×10^{-5}
Darco KB-B[a]	12×10^{-5}
Darco G-60	18×10^{-5}
Norit SA3	17×10^{-5}
Engelhard CP-97	10×10^{-5}

[a] Commercial sample was prewetted. Data have been recalculated to compensate for the mass of water.

Table 1 contains data obtained for catalysis experiments performed with wood-derived activated carbons; all samples were weakly active catalysts in the absence of palladium. It is noteworthy that Darco G-60 had the best catalytic performance. This sample is a high-purity pharmaceutical-grade product, which suggests that the catalytic activity originates from the carbon material rather than from processing impurities. The Darco KB and KB-B brands were high surface area carbons, yet they showed surprisingly low activity, even when factoring in their water content. An acetylene-based carbon black was also evaluated. It was found to be much more hydrophobic than the activated carbons, and it had negligible catalytic activity. Addition of Triton-X 100 overcame the hydrophobicity wetting problem, but it failed to increase the catalytic performance of the acetylenic carbon. Graphite, silica, and alumina showed negligible catalytic activity.

The oxidation of activated carbon surfaces has been reported to enhance the catalytic reduction of NO by NH_3 (*10*). A sample of Norit SA3 was stirred in 2 M HNO_3 overnight and then filtered and rinsed until neutral. The oxidized sample initially adsorbed more NO than the untreated material, but the rate of N_2O production on the oxidized sample dropped by 10–20% as compared to the control.

A recent report has described the role of amorphous carbon and fly ash in promoting the heterogeneous formation of N_2O from NO and SO_2 in the presence of water (*11*). Although N_2O is a product in the current anaerobic studies, we have found that the presence of O_2 arrests nitrous oxide formation (vide supra). It is unlikely that the mechanisms under consideration could contribute to atmospheric N_2O fluxes (*12–14*).

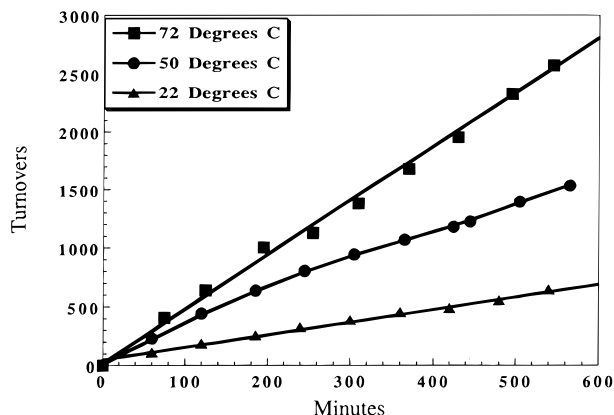**Effect of Palladium Loading on Nitric Oxide Disproportionation.** Deposition of 1% palladium on activated

FIGURE 2. Plot of the relationship between catalyst NO turnover rate and temperature of the aqueous slurry obtained with 1% Pd on activated carbon (0.1 g of catalyst, 10 mL of 3 M NaOH, 840 Torr of NO, 22 °C).

carbon produced a significant increase in catalytic performance over the untreated carbons. The activated carbon data plotted in Figure 1 represents an Engelhard carbon used in making the Sigma−Aldrich Pd/C catalysts. Increasing the palladium loading above 1% caused further increases in catalytic performance; however, the rate enhancements do not scale linearly with the absolute quantity of palladium. The best turnover efficiencies (per mole of Pd) are obtained when the palladium loading is small. This is attributed to the higher relative palladium particle surface area at low metal loadings.

The activity of the Pd^{2+}/C catalyst (prepared as described in the Experimental Section) was greater than that of the carbon alone; however, this may be attributable to the reduction of some absorbed palladium. Activated carbons are processed at high temperatures under reducing environments and are known to contain strongly reducing surface sites (15). The hydrogen-reduced Pd^0/C product exhibited much greater catalytic activity than the Pd^{2+}/C precursor, which argues for Pd^0 as the active species.

Commercial samples of Pearlman's catalyst [20% Pd(OH)₂ on carbon] yielded results comparable to the carbon controls, indicating again that adsorbed Pd^{2+} is not active as a catalyst on carbon. A suspension of Pd(0) generated by the reduction of aqueous $PdCl_2$ with CO was active catalytically, but homogeneous $PdCl_2$ was not. Additionally, a marked increase in catalysis was observed when a sample of 5% Pd(II) on $BaSO_4$ was reduced. Collectively, these results show that the most active catalysts contain Pd(0) particles. It is possible that the surface of such particles is covered with an oxide layer; however, a sample of palladium black exposed to the atmosphere for a number of years showed markedly reduced activity as compared to a freshly generated Pd(0) suspension.

The calculation of turnover rates based on palladium for the carbon-supported catalysts is complicated by the catalytic effect of activated carbon. Rather than attempt to factor out the role of the carbon (which could be as great as 25%), all NO removal observed has been assigned to the palladium. This has the advantage of facilitating cost-benefit analyses, since the palladium dopant comprises the bulk of the catalyst expense. For comparison, the turnover rates for 5% Pd on $CaCO_3$ and on alumina were determined to be 0.26 and 0.31 (mol of NO) (mol of Pd)$^{-1}$ min^{-1}, respectively. A catalyst of 0.4% Pd on alumina had a turnover rate of 2.4 mol of NO min^{-1} (mol of Pd)$^{-1}$ at 22 °C. There is no ambiguity in these values as the alumina and $CaCO_3$ blanks lacked intrinsic catalytic activity. An extensive survey of other metals has not yet been undertaken; however, commercial samples of 1% and 3% platinum on activated carbon displayed activity approximately equivalent to their palladium counterparts.
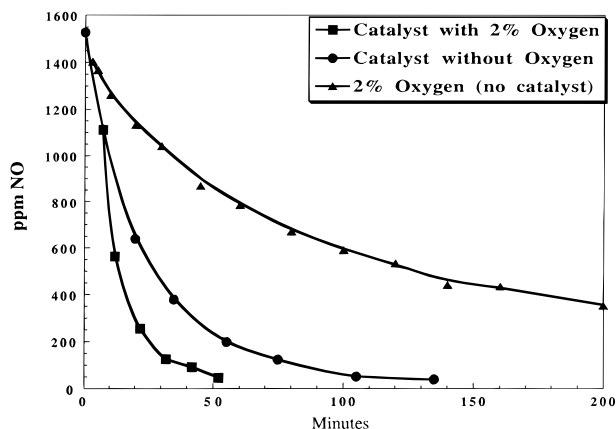
FIGURE 3. Contrasting the reactivity of low NO concentrations with 2% O₂ in the presence and absence of a 10% Pd/C catalyst. The disproportionation reaction of NO with the catalyst in the absence of 2% O₂ is included for comparison (1.0 g of catalyst, 100 mL of 1 M NaOH, 22 °C).

Figure 2 contains a plot that shows the effects of warming the aqueous slurry. The room temperature (22 °C) rate of NO disproportionation with a sample of 1% Pd/C was (1.1 × 10^{-4} mol of NO) min^{-1} (g of catalyst)$^{-1}$. These values increased to (2.6 × 10^{-4} mol of NO) min^{-1} (g of catalyst)$^{-1}$ at 50 °C and (4.7 × 10^{-4} mol of NO) min^{-1} (g of catalyst)$^{-1}$ at 72 °C. These values translate to turnover rates of 1.1, 2.6, and 4.7 mol of NO min^{-1} (mol of Pd)$^{-1}$, respectively.

Catalytic Oxidation of Nitric Oxide with O₂. Flue gases typically contain 2−15% O₂, and the performance of many catalysts are impaired significantly in aerobic environments. Nitric oxide undergoes a third-order gas-phase reaction with O₂ that is fast at high NO concentrations (eq 2a), but it becomes slow as nitric oxide levels drop into the low ppm range (14).

$$2NO + O_2 \rightarrow 2NO_2 \text{ rate} = k_{air}[NO]^2[O_2] \qquad (2a)$$
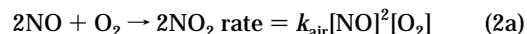
A similar reaction (eq 2b) takes place under aqueous conditions, except the product is nitrite rather than nitrogen dioxide (16, 17).

$$4NO + O_2 + 2H_2O \rightarrow$$
$$4NO_2^- + 4H^+ \text{ rate} = k_{aq}[NO]^2[O_2] \quad (2b)$$
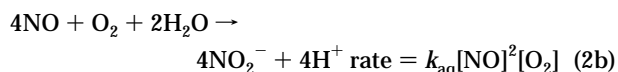
It has been observed that k_{aq} is greater than k_{air} by a factor of 400; however, the small Henry's constants for NO and O₂ render the observed nitric oxide loss rates approximately equal (18).

A closed-loop recirculating reactor was used to study the oxidation of NO at concentrations below 6000 ppm. Blank reactions were used to quantify the gas-phase and aqueous-phase reactions (eqs 2a and 2b) with 2% O₂ in the headspace. Figure 3 shows that the anaerobic Pd/C catalyst removes NO significantly faster than the combined gas- and aqueous-phase reactions with O₂. When the Pd/C catalyst was substituted with activated carbon, the rate of NO removal was indistinguishable from the background reaction with oxygen. When 2% oxygen was added along with the Pd/C catalyst, the rate of NO removal was markedly faster than when the catalyst was absent. These results suggest that activated carbon is not an efficient catalyst for the oxidation reaction but that palladium particles are highly effective. During the experiment depicted in Figure 4, the reaction was carried out under anaerobic conditions for 30 min, at which time the atmosphere was enriched with 2% O₂. It can be seen that the NO depletion rate is dramatically enhanced
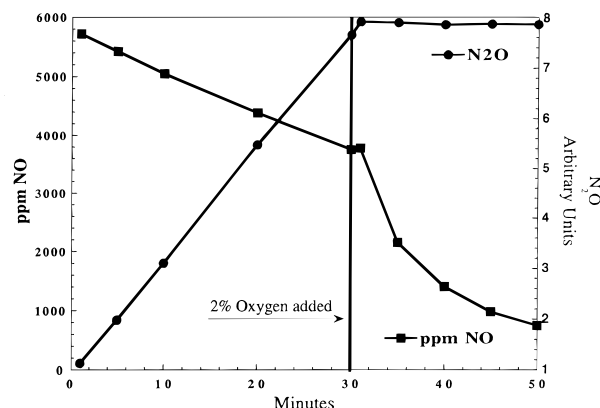
FIGURE 4. Effects of introducing O_2 into the headspace during the reaction of NO over a 10% Pd/C catalyst. Two percent O_2 was added after 30 min, as indicated by the solid vertical line (1.0 g of catalyst, 100 mL of 1 M NaOH, 22 °C).
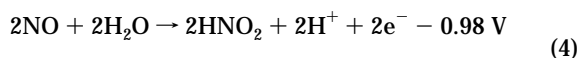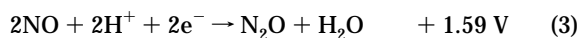
and that the introduction of oxygen completely eliminates N_2O production. The significance of this is discussed in detail below.
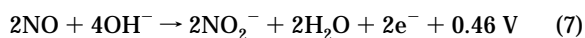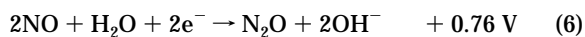
Discussion

Stoichiometry and Mechanism. Quantitative analyses [GC analysis of NO and N_2O headspace gases (*19*), UV determination of NO_2^-, and titration of filtered reaction solutions with standardized HCl] have established that under anaerobic conditions the aqueous disproportionation of nitric oxide proceeds according to the stoichiometry of eq 1. The measured stoichiometry of NO_2^- was 1.89−1.97 as ratioed to the NO consumed. The NO:N_2O stoichiometry ratio was often low at short reaction times but ranged between 3.5 and 4.4 for reactions near completion. Gas adsorption by the activated carbon support led to an immediate rapid uptake of gas-phase NO (a gas with otherwise low aqueous solubility) before significant N_2O formed, and this accounts for the low initial ratios.

This stoichiometry is obeyed by the disproportionation reactions catalyzed by both activated carbon and by palladium-loaded activated carbon. Electrochemical half-cell reduction potentials (eqs 3−8) show that nitric oxide disproportionation directly to nitrous oxide and nitrite should be thermodynamically spontaneous at pH values between 0 and 14.
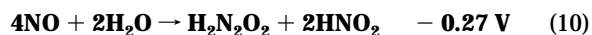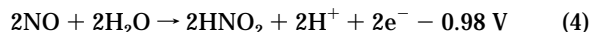
Acidic Conditions

$$2NO + 2H^+ + 2e^- \rightarrow N_2O + H_2O \qquad + 1.59 \text{ V} \qquad (3)$$

$$2NO + 2H_2O \rightarrow 2HNO_2 + 2H^+ + 2e^- \quad - 0.98 \text{ V} \qquad (4)$$

$$\mathbf{4NO + H_2O \rightarrow N_2O + 2HNO_2} \qquad + \mathbf{0.61 \text{ V}} \qquad (5)$$

Basic Conditions

$$2NO + H_2O + 2e^- \rightarrow N_2O + 2OH^- \qquad + 0.76 \text{ V} \qquad (6)$$

$$2NO + 4OH^- \rightarrow 2NO_2^- + 2H_2O + 2e^- \quad + 0.46 \text{ V} \qquad (7)$$

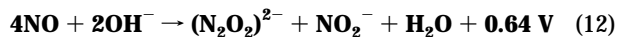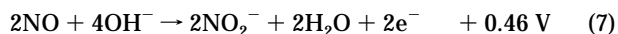$$\mathbf{4NO + 2OH^- \rightarrow N_2O + 2NO_2^- + H_2O + 1.22 \text{ V}} \qquad (8)$$

That the catalytic disproportionation reaction occurs only in basic media suggests that additional complexity may be associated with the mechanism. One likely role of the catalysts is to bring NO molecules into close association on the surface as diamagnetic NO dimers. A two-electron

reduction of this dimer would result in the formation of a bound hyponitrite $(N_2O_2)^{2-}$ intermediate. Redox chemistry based on the intermediacy of a hyponitrite species is thermodynamically favorable under basic conditions, but it becomes unfavorable in acidic media (eqs 10 and 12).

Acidic Conditions

$$2NO + 2H^+ + 2e^- \rightarrow H_2N_2O_2 \qquad + 0.71 \text{ V} \qquad (9)$$

$$2NO + 2H_2O \rightarrow 2HNO_2 + 2H^+ + 2e^- \quad - 0.98 \text{ V} \qquad (4)$$

$$\mathbf{4NO + 2H_2O \rightarrow H_2N_2O_2 + 2HNO_2} \qquad \mathbf{- 0.27 \text{ V}} \qquad (10)$$

Basic Conditions

$$2NO + 2e^- \rightarrow (N_2O_2)^{2-} \qquad + 0.18 \text{ V} \qquad (11)$$

$$2NO + 4OH^- \rightarrow 2NO_2^- + 2H_2O + 2e^- \qquad + 0.46 \text{ V} \qquad (7)$$

$$\mathbf{4NO + 2OH^- \rightarrow (N_2O_2)^{2-} + NO_2^- + H_2O + 0.64 \text{ V}} \qquad (12)$$

The Nernst equation was used to estimate $E = 0$ at pH 6.3. This agrees with the experimental results, which show a dramatic decrease in rate between pH 7.5 and pH 6.5. Hyponitrite is known to decompose spontaneously to nitrous oxide by eq 13, so it is a reasonable precursor to N_2O formation (*20*).

$$(N_2O_2)^{2-} + H_2O \rightarrow N_2O + 2OH^- \qquad (13)$$
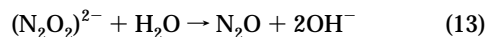
It has been reported that the formation of $(NO)_2$ dimers within nanoporous sites on activated carbon fibers (ACFs) can disproportionate nitric oxide directly to N_2O and NO_2 at room temperature (*21*). The reaction catalysis was attributed to the nature of the nanopore environment. The catalytic redox chemistry described herein is markedly faster and is not restricted to such specialized surfaces. A recent report suggests that ruthenium within the nanoporous sites of (ACFs) strongly promotes NO reduction to N_2 (*22*); however, the reported results did not show whether ruthenium was performing as a catalyst or a stoichiometric reductant. Turnover numbers exceeding 2000 were recorded for the 1% Pd/C catalyst in the present study, which unambiguously establishes the catalytic nature of the reactions.

Figure 5 depicts a hypothetical model of heterogeneous catalysis consistent with the observed results. Adsorbed NO molecules are brought into close association, either in carbon micropores or on the palladium surface, and reduced to hyponitrite. It is possible that the palladium serves as a bulk electron reservoir, although the reducing equivalents are ultimately provided by the oxidation of nitric oxide to nitrite. Evidence that supports palladium as an intermediate in the redox scheme is provided by the observation that a small amount of Pd(II) (6−10% of the total palladium) was leached off of a 10% Pd/C catalyst during the course of catalytic NO disproportionation. Palladium(II) was not detected when the catalyst was treated under the same conditions in the presence of N_2 rather than NO. This suggests that the palladium may be involved in repeated oxidation/reduction cycles. It is known that Pd(0) will react with NO to yield N_2O (eq 14) (*23*).

$$Pd(0) + 2NO + H_2O \rightarrow Pd^{2+} + N_2O + 2OH^- \qquad (14)$$
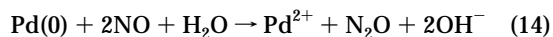
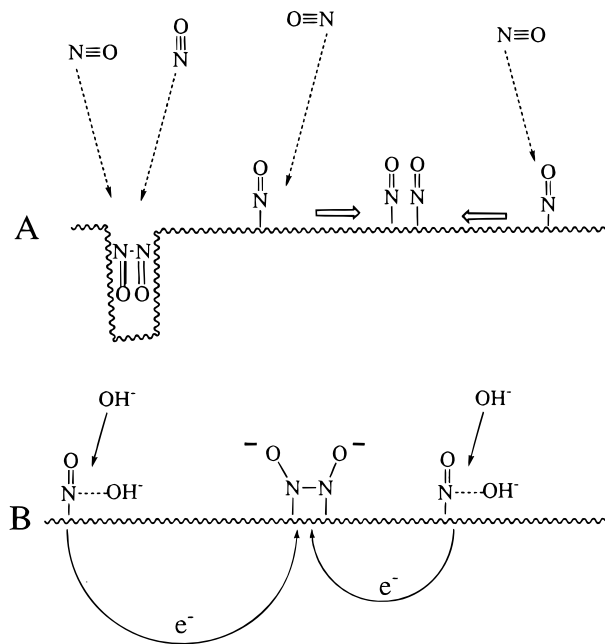The palladium catalysts reported here were not poisoned by the addition of 200−300 Torr of SO_2 to the gaseous

FIGURE 5. Model for the heterogeneous catalytic reduction of NO in base. (A) $(NO)_2$ dimers form on the surface either by the effects of microporosity or by migration. (B) Attack of hydroxide on bound NO forms NO_2^- and liberates electrons into the bulk catalyst, ultimately reducing $(NO)_2$ dimers to bound hyponitrite.

FIGURE 6. Plot of the relationship between catalyst NO turnover rate (obtained from N_2O appearance during the initial stage of reaction) and the NO partial pressure. The reaction used 10% Pd on activated carbon (0.1 g of catalyst, 10 mL of 3 M NaOH, 22 °C). The plateau above 500 Torr of NO suggests that the rates in this region are limited by mass transfer of NO into the solution or by saturation of NO binding sites.

reactants (the SO_2 rapidly dissolved and reacted with the NaOH solution) nor by 0.2 M aqueous sodium sulfite and sulfate. Such conditions poison many other NO_x control catalysts, but the strongly basic reaction conditions employed with the aqueous slurry catalysts prevent this. With added sodium sulfite, the reaction rate for NO removal even increased slightly, as aqueous sulfite reacts directly with NO.

Activated carbons are well-known as an absorbent of VOCs and other gaseous pollutants. The wet scrubbing reactor's capacity for eliminating NO_2 and SO_x, and an adsorptive catalytic mechanism for NO removal, may offer a new approach to the removal of pollutants from stack gases. However, the present catalytic system has far too low activity to be of practical use. Turnover data were determined from experiments performed at high NO concentrations. At pressures above 500 Torr, the rate of depletion is essentially invariant, while at lower pressures it decreases with a first-order dependence (Figure 6) on NO pressure (p_{NO}). The plateau above 500 Torr suggests mass-transfer limitation of NO uptake into the stirred solution or saturation of catalyst binding sites. The turnover rate for a 1% Pd/C catalyst was 0.03 (mol of NO) (mol of Pd)$^{-1}$ min^{-1} over the range 5000−1000 ppm NO. This is consistent with the anticipated 2 orders of magnitude decrease in rate from the high p_{NO} reactions. For comparison, the maximum turnover frequency of a copper-doped ZSM-5 zeolite sample was 1.5 (mol of NO) (mol of Cu)$^{-1}$ min^{-1} at 750 K (*24*). This experiment was run at 4% NO in He under 1.7 atm of pressure (i.e., approximately 50 Torr of NO). Given the first-order dependence, the turnover frequencies of the current Pd^0 catalyst under comparable pressures can be estimated at 0.11, 0.26, and 0.47 (mol of NO) (mol of Pd)$^{-1}$ min^{-1} at 295, 321, and 345 K, respectively.

The possibility of using the aqueous catalytic process for NO removal would be contingent on the elimination of nitrous oxide generation, for N_2O is now recognized as a potential atmospheric pollutant (*12−14*). Fortunately, the presence of O_2 in the gas stream eliminates nitrous oxide formation (Figure 4). A detailed analysis of oxygen's role in the reaction is not yet complete; however, it seems plausible
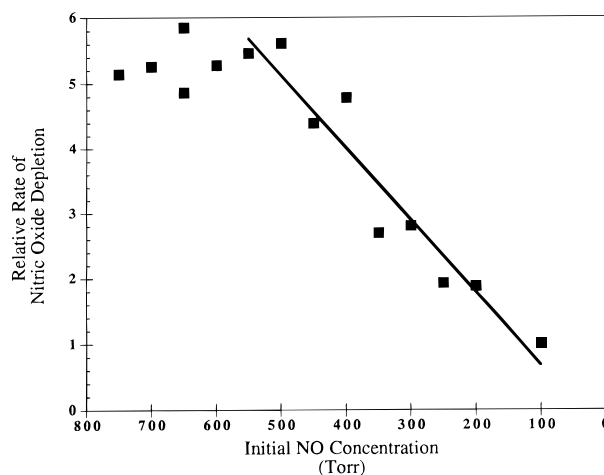
that the oxygen supplants the nitric oxide dimer (Figure 5B) as the surface electron acceptor. This would result in all the NO being oxidized to nitrite, by analogy to reaction 2. An alternative explanation for the cessation of nitrous oxide production in the presence of oxygen would involve secondary oxidation of a bound hyponitrite intermediate by O_2, which occurs faster than its decomposition to N_2O. Insufficient evidence exists to distinguish between these two possible reactions pathways, and it is possible that they may both be active to some degree in alkaline aqueous media. Further mechanistic studies of the surface redox processes by electrochemical methods is in progress.

Acknowledgments

Supporting Information Available

Seven figures and captions showing the apparatus used for recirculation experiments, a comparison of catalytic efficiency as a function of palladium loading on carbon, a comparison of catalytic activity of Pd(0) and Pd^{2+} on carbon catalysts, a comparison of catalytic activity of Pd(0) and Pd^{2+} on barium sulfate catalysts, a plot of product (N2O) formation versus pH for a palladium on carbon catalyst, and the rate of production formation for a dry Pd^0/C catalyst impregnated with NaOH (8 pp) will appear following these pages in the microfilm edition of this volume of the journal. Photocopies of the Supporting Information from this paper or microfiche (105 × 148 mm, 24× reduction, negatives) may be obtained from Microforms Office, American Chemical Society, 1155 16th St. NW, Washington, DC 20036. Full bibliographic citation (journal, title of article, names of authors, inclusive pagination, volume number, and issue number) and prepayment, check or money order for $19.50 for photocopy ($21.50 foreign) or $12.00 for microfiche ($13.00 foreign), are required. Canadian residents should add 7% GST. Supporting Information is also available via the World Wide Web at URL http://www.chemcenter.org. Users should select Electronic Publications and then Environmental Science and Technology under Electronic Editions. Detailed instructions for using this service, along with a description of the file

formats, are available at this site. To down-load the Supporting Information, enter the journal subscription number from your mailing label. For additional information on electronic access, send electronic mail to si-help@acs.org or phone (202)872-6333.

Literature Cited

(1) Summers, J. C.; Sawyer, J. E.; Frost, A. C. *The 1990 clean air act and catalytic emission control technology for stationary sources*; Summers, J. C., Sawyer, J. E., Frost, A. C., Eds.; American Chemical Society: Washington, DC, 1992; Vol. 495, pp 98−114.

(2) Armor, J. N. *NO$_x$ removal: an overview*; Armor, J. N., Ed.; American Chemical Society: Washington, DC, 1994; Vol. 552, pp 2−6.

(3) Iwamoto, S.; Shimizu, S.; Inui, T. *Stud. Surf. Sci. Catal.* **1994**, *84*, 1523−1530.

(4) Iwamoto, M.; Yahiro, H. *Catal. Today* **1994**, *22*, 5−18.

(5) Centi, G.; Passarini, N.; Perathoner, S.; Riva, A. *Contemporaneous removal of SO$_2$ and NO from flue gas using a regenerable copper-on-alumina sorbant-catalyst*; Centi, G., Passarini, N., Perathoner, S., Riva, A., Eds.; American Chemical Society: Washington, DC, 1994; Vol. 552, pp 233−249.

(6) Liu, D. K.; Shen, D. X.; Chang, S. G. *Environ. Sci. Technol.* **1991**, *25*, 55−60.

(7) Pereira, C. J.; Amiridis, M. D. *NO$_x$ Control from Stationary Sources*; Pereira, C. J., Amiridis, M. D., Eds.; Washington, DC, 1995; Vol. 552, pp 1−13.

(8) Pham, E. K.; Chang, S. G. *Nature* **1994**, *369*, 139−141.

(9) Chang, S. G.; Liu, D. K. *Nature* **1990**, *343*, 151−153.

(10) Ku, B. J.; Lee, J. K.; Park, D.; Rhee, H.-K. *Ind. Eng. Chem. Res.* **1994**, *33*, 2868−2874.

(11) Pires, M.; Van der Bergh, H.; Rossi, M. J. *J. Atmos. Chem.* **1996**, *25*, 229−250.

(12) Cicerone, R. J. *J. Geophys. Res.* **1989**, *94*, 18265.

(13) Thiemens, M. H.; Trogler, W. C. *Science* **1991**, *251*, 932−934.

(14) Trogler, W. C. *J. Chem. Educ.* **1995**, *72*, 973−976.

(15) Cameron, D. S.; Cooper, S. J.; Dodgson, I. L.; Harrison, B.; Jenkins, J. W. *Catal. Today* **1990**, *7*, 113−137.

(16) Wink, D. A.; Darbyshire, J. F.; Nims, R. W.; Saavedra, J. E.; Ford, P. C. *Chem. Res. Toxicol.* **1993**, *6*, 23−27.

(17) Awad, H. H.; Stanbury, D. M. *Int. J. Chem. Kinet.* **1993**, *25*, 375−381.

(18) Pires, M.; Rossi, M. J.; Ross, D. S. *Int. J. Chem. Kinet.* **1994**, *26*, 1207−1227.

(19) MacNeil, J.; Zhang, H.-T.; Berseth, P.; Trogler, W. *J. Am. Chem. Soc.* **1997**, *119*, 9738−9744.

(20) Greenwood, N. N.; Earnshaw, A. *Chemistry of the Elements*, 1st ed.; Pergamon Press: New York, 1984.

(21) Li, G. X.; Nishi, Y.; Ozeki, S.; Kaneko, K. *Carbon* **1994**, *32*, 1186−1188.

(22) Nishi, Y.; Suzuki, T.; Kaneko, K. *J. Phys. Chem. B* **1997**, *101*, 1938−1939.

(23) MacNeil, J. H.; Berseth, P. A.; Bruner, E. L.; Perkins, T. L.; Wadia, Y.; Westwood, G.; Trogler, W. C. *J. Am. Chem. Soc.* **1997**, *119*, 1668−1675.

(24) Zhang, Y.; Flytzani-Stephanopoulos, M. *Catalytic decomposition of nitric oxide over promoted copper-ion-exchanged ZSM-5 zeolites*; Zhang, Y., Flytzani-Stephanopoulos, M., Eds.; American Chemical Society: Washington, DC, 1994; Vol. 552, pp 7−21.